A SYNCHROPHASOR ESTIMATION ALGORITHM FOR THE MONITORING OF ACTIVE DISTRIBUTION NETWORKS IN STEADY STATE AND TRANSIENT CONDITIONS

M. Paolone, A. Borghetti, C. A. Nucci
University of Bologna
mario.paolone@unibo.it, alberto.borghetti@unibo.it, carloalberto.nucci@unibo.it

Abstract –The paper presents a PMU prototype specifically developed for active distribution network applications. The paper describes the method developed to accurately measure the synchrophasors, its implementation into a real-time microcontroller and the relevant characterization in both steady state and transient conditions. Concerning these last points, the paper presents a test procedure suitably conceived to characterize the PMU with both steady state – single tone and distorted – and frequency-varying signals simulating power systems electromechanical transients. The results show that the developed PMU exhibits high accuracy levels that are not modified by the harmonic distortion of the reference signal and by its frequency-varying transient behavior and compatible with their use into power distribution networks.

Keywords: phasor measurement units, synchrophasors, PMUs characterization, active distribution networks, real time monitoring.

1 INTRODUCTION

The evolution of distribution networks from passive to active power systems is determining major changes in their operational procedures [1] and one of the main involved aspects is the network monitoring [2]. In particular, the above issues call for a massive use of advanced and smarter monitoring tools that result into faster and reliable real-time state estimation of these networks. One of the most promising technologies in this field is certainly represented by the distributed measurement of synchrophasors based on the use of phasor measurement units (PMUs) [2,3].

As known, PMUs provide the measurements of node voltage and/or branch current phasors synchronized with a common time reference (typically the one provided by the global positioning system UTC-GPS) [2-4]. The increasing use of data provided by PMUs in the real-time operation of power systems, the availability of accurate timing devices, and of advanced signal processing techniques and telecommunication infrastructures, has resulted in the development of PMUs characterized by increasing accuracy levels [4].

Examples of PMU use within the context of power distribution networks operation have been presented in the literature in the following fields: protection functions, such as loss of main (e.g. [5]), fault event monitoring [6], state estimation (e.g. [7]), synchronous islanded operation [8] and for power quality monitoring (e.g. [9]). As these application fields cope with both steady state and transient conditions, it is worth noting that synchrophasor estimation algorithms should be robust against the transient behavior of networks phasor quantities [10,11].

Within this context, and on the basis of [12], the paper presents an improved synchrophasor estimation algorithm suitably developed for wide area monitoring of distribution networks. The paper shows the peculiar characteristics of such an algorithms that allow to achieve: (i) low values of synchrophasors estimation uncertainties, (ii) high rejection of harmonic components different from the fundamental one; (iii) maintain uncertainty levels to values not modified by the transient behavior of frequency-varying phasors.

Concerning this last aspect, the paper focuses on the PMU performance assessment with reference to both steady-state and transient conditions and, to this purpose, presents a specific characterization procedure.

The structure of the paper is the following: section II illustrates the synchrophasor estimation algorithm as well as its implementation into a PMU prototype which hardware is composed by an embedded real-time microcontroller; section III presents the procedures developed to characterize the PMU prototype in both steady state and transient conditions and, also, the relevant experimental results. Section IV concludes the paper discussing the characteristics of the developed device.

2 SYNCHROPHASOR ESTIMATION ALGORITM

Synchrophasor estimation algorithms proposed in the literature are essentially based on the Discrete Fourier Transform (DFT) applied to quasi-steady state signals that represents node voltages and/or branch current waveforms. These DFT-based algorithms can be grouped into one-cycle DFT estimators, and fractional-cycle DFT estimators performing recursive and non-recursive updates (e.g. [4,13]). As an example, the measurement procedure proposed in [14] is based on a sample reallocation procedure and on the DFT application using both fixed and adjustable-length time windows. The obtained standard deviation of the error distribution of the synchrophasor phase estimates is in the order of 0.3 mrad.

Non-DFT algorithms for the synchrophasor estimation (e.g. based on the least-square method) have been also proposed in literature in order to improve the accuracy of phasor and frequency measurements (e.g. [15]).

Within this context, the algorithm presented by the Authors belongs to the DFT algorithms and has been conceived in order to: (i) allow the use of PMU in active distribution networks and (ii) keep the synchrophasor measurement accuracy within specific limits even in presence of distorted signal waveforms and electromechanical transients.

Concerning point (i), it is worth mentioning that, compared to transmission networks, active distribution networks are characterized by reduced line lengths and limited power flows. With reference to the use of node voltage synchrophasors for the network state estimation, these characteristics result, in general, into very small phase differences between node voltage phasors (generally in the order of tens of mrad or less). These characteristics, in view of what discussed in the Appendix, call for the development of PMU devices characterized by synchrophasor phase uncertainty well below the limits provided by the IEEE Std. C37.118 [3].

Concerning point (ii), it is worth noting that distribution networks are characterized by distortion levels much higher than those of transmission networks. Additionally, as active distribution networks are expected to be operated even islanded from main transmission networks, PMUs appear a useful tool to support distribution system operators during the islanding and reconnection maneuvers [12]. In this respect, the application of PMU to monitor electromechanical transients, in general characterized by non-negligible deviations from the nominal frequency, could involve, as discussed in [4,10,11], an important misestimation of synchrophasors phases and frequencies. This specific aspect calls for the following additional requirements: (i) use of consecutive independent observation windows in order to reach an accurate estimate of the electromechanical transient frequencies; (ii) estimation of the frequency using a sufficient number of phase angle measurements with a reasonable span of 3-6 cycles of the nominal frequency and (iii) frequency estimation with the same time-tag used for the phasor estimation.

2.1 Synchrophasor estimation algorithm

Traditional synchrophasor estimation algorithms based on the use of the DFT perform, in general, the synchrophasor measurement directly from the output of the DFT applied to a signal typically sampled with a rate in the order of few kHz. On the other hands, the algorithm proposed by the Authors in [12], although still based on the use of the DFT, makes use of a two step approach in which the first step consists of a DFT analysis of the input signal and the second step of a time-domain analysis of the reconstructed time-domain signal that corresponds to the fundamental-frequency tone. The peculiar characteristic of the first step is that it allows the identification of the fundamental frequency tone by using the procedure proposed in [16]. Such a procedure provides accurate results in case PMUs use high sampling frequencies (namely, in the order of 50-100 kHz). In what follows a brief description of the synchrophasor estimation algorithm is given.

Let $s(t)$ the PMU input signal expressed as

$$s(t) = \tilde{s} + \sum_{h=1}^{n} s_h \cos\left(h\omega_0 + \varphi_h\right) + \varepsilon_t \qquad (1)$$

where: $\tilde{s}$ is the DC component within the sampled time window T, s_h and φ_h are the amplitude and phase of the h-th harmonic component, and ε_t is the Gaussian noise. Such a time signal is sampled by the PMU each $\Delta t = T/N = 1/f_s$ into a time window T sufficiently short (in our case 80 ms) so that the signal can be assumed stationary within T. As known, the DFT of (1) with the above sampling parameters is

$$G\left(k\Delta f\right) = \sum_{h=1}^{n} S_h \; D_N\left[\left(k\Delta f - f_h\right)T\right] \qquad (2)$$

where N is the number of samples, $\Delta f = 1/T$, $\Delta t = T/N$, $k = 0,\ldots(N/2)-1$, S_h and f_h are the amplitude and frequency of tone h, whilst D_N is the so-called Dirichlet kernel defined by

$$D_N\left(\vartheta\right) = \frac{\sin\left(\pi\vartheta\right)}{N\sin\left(\pi\vartheta/N\right)} e^{-\pi i \vartheta\frac{(N-1)}{N}} \qquad (3)$$

In case $s(t)$ is sampled with a sampling frequency so that the Nyquist frequency, $f_s/2$, can be assumed to be much larger than the maximum frequency component of $s(t)$, the aliasing effects on the signal can be disregarded as well as the presence of relevant filters. In view of the typical frequency values of highest spectrum components that characterize distorted voltage and current signals of distribution networks (i.e. not larger than 10 kHz), the above mentioned advantage has justified the adoption of a sampling frequency in the order of 100 kHz. As discussed in what follows, the adoption of such high sampling frequency also have a further advantage in the identification of the fundamental frequency tone.

The identification of the fundamental frequency tone of $s(t)$ associated to the identification of the synchrophasor, faces the following two main problems:

a) spectral leakage effects caused by the finite length of time window T;
b) identification of the correct frequency value that may fall between two subsequent frequency values provided by the DFT.

The algorithm copes with the issue (a) by applying the convolution to the sampled data with the Hanning window:

$$G_H\left(k\Delta f\right) = \sum_{h=1}^{n} S_h H_N\left[\left(k\Delta f - f_h\right)T\right] \qquad (4)$$

where H_N is the Fourier transform of the Hanning windowed data.

Concerning point (b), in general, the true frequency f_0 of the fundamental frequency tone can be expressed as a function of the discrete DFT frequency discretization step Δf:

$$f_0 = \left(m + \Delta bin\right)\Delta f \qquad (5)$$

where Δbin ($0 \le \Delta bin < 1$) is the deviation of f_0 from the multiple integer DFT frequency $m\Delta f$ (m=1,2,…). In (5), m and $m+1$ indicate the two DFT tones that delimit the interval in which f_0 is assumed to be.

As discussed in [16], since the number N of samples

per time window T is very large[1], the two following approximation can be applied: (i) the sine function in the denominator of the Dirichlet kernel (3) can be approximated by its argument and (ii) $e^{-\pi i\frac{N-1}{N}} \approx -1+\frac{\pi i}{N}$.

As shown in [16], these assumption led to a linear expression of $G_H(k\Delta f)$ as a function of Δbin and, as a consequence, this last quantity can be approximated as a function of the highest and the second highest tone magnitudes, respectively a and b, in the discrete spectrum of G_H:

$$\Delta bin = \pm\frac{a-2b}{a+b} \qquad (6)$$

The complex amplitude of the fundamental frequency tone S_1 at f_0 is estimated as

$$S_1 = \frac{2\pi\ \Delta bin\left(1-\Delta bin\right)}{\sin\left(\pi\Delta bin\right)} e^{-\pi i\Delta bin}\left(1+\Delta bin\right) G_H\left(m\Delta f\right) \qquad (7)$$

The estimation of S_1 provides the value of the fundamental frequency tone amplitude s_1 together with its phase φ_1. Once amplitude s_1, phase φ_1 and Δbin are known, the proposed algorithm performs a further step in order to improve the estimation of the synchrophasor phase φ_1. Indeed, the synchrophasor phase is known with an accuracy that, neglecting the uncertainties due to the DFT, is correlated to the sampling time step Δt. In particular, such an uncertainty corresponds, for an f_s=100 kHz and a rated system frequency of 50 Hz, to π mrad (0.18 deg), a value that, in view of what illustrated in the Appendix, is too large. Therefore, the algorithm applies the following procedure. The first step consists into the reconstruction into the time-domain of the fundamental frequency tone given by

$$s_1\left(t\right) = S_1\cos\left(2\pi f_0 t+\varphi_1\right) \qquad (8)$$

In case the sampling of $s(t)$ is triggered in correspondence of rise of the time reference pulse per second (PPS) signal, Fig. 1 shows the procedure to improve the calculation the synchrophasor phase: the dash-point line represents a generic signal $s(t)$, the continuous line the time-domain reconstructed fundamental frequency tone $s_1(t)$ and the dashed line the PPS signal.

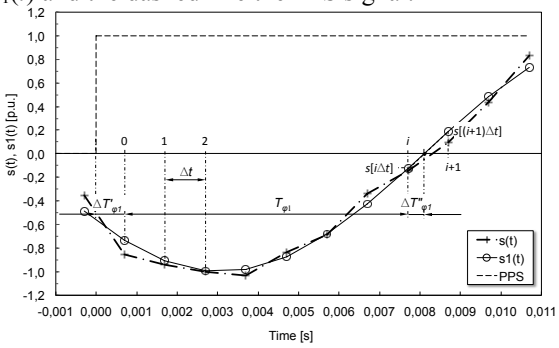

Figure 1: Reconstructed signal $s_1(t)$ and redefinition of its phase.

[1] Such a condition satisfied by the adopted sampling frequency (i.e. 100 kHz) that is much larger than the fundamental tone frequency f_0 (i.e. 50-60 Hz).

By making reference to Fig. 1, the value of the synchrophasor phase φ_1 is further estimated as follows:

$$\varphi_1 = \frac{3}{2}\pi - 2\pi f_0\left(T_{\varphi 1}+\Delta T'_{\varphi 1}+\Delta T''_{\varphi 1}\right) \qquad (9)$$

where:

- $T_{\varphi 1} = i\Delta t$;
- $\Delta T'_{\varphi 1} = k\frac{1}{f_{FGPA}^{clock}}$;
- $\Delta T''_{\varphi 1} = \Delta t\frac{s\left[i\Delta t\right]}{\left|s\left[i\Delta t\right]-s\left[\left(i+1\right)\Delta t\right]\right|}$.

The estimation of $\Delta T'_{\varphi 1}$ is realized by means of a counter that estimates (with the pointer k) the time interval between the PPS rise and the first acquired sample of the $s(t)$. This counter is associated to the clock frequency of the FPGA, f_{FGPA}^{clock}, of the hardware where the algorithm is implemented. Further details on the implementation issues are given in the following subsection. It is also worth mentioning that the term $3/2\pi$ in (9) is needed in order to estimate the synchrophasor phase angle in agreement with the time reference defined in [3].

2.2 Microcontroller implementation

The algorithm has been implemented into a National Instruments Compact-Rio embedded real-time microcontroller equipped with an FPGA (Field Programmable Gate Array) bus. The microcontroller is characterized by a 400 MHz real-time processor with 2 GB nonvolatile storage, 128 MB DRAM memory linked with a 3 Mgate FPGA. The sampling of the voltage waveforms is realized by means of three parallel 16-bits digitizers, characterized by a signal input dynamic of ± 10 V, that synchronously operate at the FPGA level together with the availability of the UTC-GPS time frame provided by an IRIG-B GPS unit characterized by a time uncertainty of 100 ns.

The structure of the microcontroller implementation is illustrated in Fig. 2.

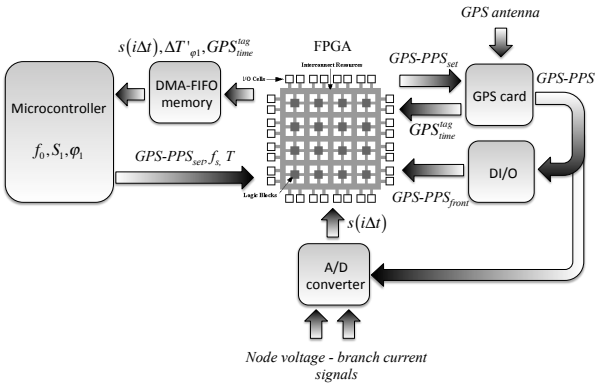

Figure 2: Implementation of the synchrophasor estimation algorithm into the NI CompactRio embedded microcontroller.

As it can be seen from Fig. 2, the microcontroller sends to the FPGA the set point of the following quantities:

- sampling frequency f_s;
- observation time window T;
- number of GPS-PPS.

The FPGA forward the number of PPS[2] to the GPS card that generates a PPS signal sent to both the 16-bits A/D converter and to the digital I/O card. These connections allow to trigger the start of the $s(t)$ sampling in correspondence of the PPS front (for a duration corresponding to the observation time window T). At the same time, the PPS front sent to the digital I/O card allows to trigger the start of the FPGA counter running at the FPGA clock frequency (f_{FGPA}^{clock}) which, for the adopted hardware, is equal to 40 MHz. This counter is stopped in correspondence of the first sample of $s(t)$ allowing the calculation of $\Delta T'_{\varphi 1}$. The digitalized sampled data, as well as the GPS time tag, are inserted into a DMA-FIFO memory and retrieved by the microcontroller in order to perform the above-described synchrophasor estimation algorithm.

3 PROCEDURES FOR PMU CHARACTERIZATIONS IN STEADY STATE AND TRANSIENT CONDITIONS

Performances of PMUs are generally inferred by means of reference-signals with accuracies, in terms of amplitude and phase, need to be much higher of the one of the PMU under test (e.g. [17]). In this respect, the experimental characterization of the developed PMU has been carried out by using reference waveforms generated by means of a GPS-synchronized function generator based on the PXI (PCI eXtensions for Instrumentation) architecture. In particular, the system is composed by a National Instruments PXI 1042Q chassis on which the following devices are connected: (i) NI PXI-5441 arbitrary waveform generator, (ii) NI PXI-6682 GPS IRIG-B timing and synchronization module, (iii) NI PXI-6281 high accuracy data acquisition board and (iv) NI PXI-8110 high-performance Intel Core 2 Quad Q9100-based embedded controller. The characteristics and accuracies of each device are reported below:

i) PXI-5441: 16-bit resolution, output generation frequency of 100 MS/s, carrier frequencies with 355 nHz resolution and PXI time synchronization skew < 20 ps;
ii) PXI-6682: onboard 10 MHz clock with skew of 1 ppm, GPS synchronization accuracy ±100 ns with 13 ns standard deviation;
iii) PXI-6281: 18-bit resolution inputs at 500 kS/s sampling rate, analog input accuracy 980 μV over ±10 V input range.

The PXI architecture of the system allows to share 10 MHz TTL clocks, transmitted on equal-length traces, providing skew less than 1 ns between the different devices. The accuracy of the 10 MHz clock is typically less than 25 ppm. Fig. 3 shows the structure of the PMU reference signal generator. The GPS device acts as reference clock generating a number of GPS synchronized PPS on the PXI bus. The number of PPS corresponds to the frequency of the reference signal. The arbitrary function generator produces, in correspondence of the rise of the GPS-PPS and with a frequency of 100 MHz, a single period of the reference waveform that is sent to both the PMU under test and to the high-accuracy DAQ board PXI-6281. The measurement performed by this last device is also triggered by the GPS-PPS signal shared on the PXI bus so that it provides the true value of the synchrophasor amplitude.

The architecture of the reference signal generator allows, therefore, generating both steady state and transient signals (both characterized by single tone and distorted waveforms) by simply controlling the number of PPS and the waveshape of the generated waveform.

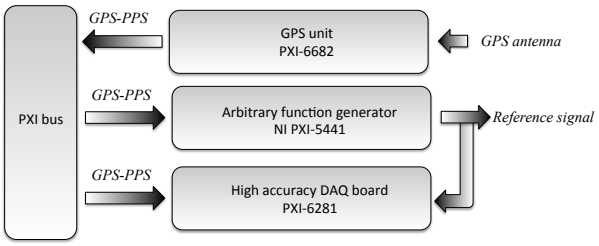

Figure 3: Structure of the PMU reference signal generator.

3.1 Steady state conditions

The experimental characterization reported in this sub-section refers to periodical signals characterized by spectrum components with constant frequency. In particular, two cases have been analyzed, namely: (i) single-tone (50 Hz) and (ii) distorted signals. Concerning this last case, the reference signal has been generated with spectrum components equal to the limit values provided by the standard EN 50160 [18]. Fig. 4 shows the cumulative statistical distribution of the synchrophasor phase error concerning both cases and obtained with reference to 20.000 synchrophasor estimations. As it can be seen, the two distributions are normal. The distributions of the other errors (i.e. RMS, Frequency and TVE) are not reported but the main statistical data are summarized in Table I. In particular, as defined in [19], the standard deviations reported in Table I correspond to the so-called standard uncertainty and prove that the developed PMU are compatible with the requirements of power distribution networks applications.

It is worth noting that, compared with the results obtained in [12], the one here reported shows an improvement of the performances of the PMU-prototype essentially due to the correction on the synchrophasor phase estimation. Additionally, the PMU accuracy is not affected by the presence of the harmonic distortion of the reference signals, which, as above discussed, is an essential requirement for PMUs application in distribution networks.

[2] It is worth noting that the number of PPS corresponds to the number of synchrophasor estimation per second.

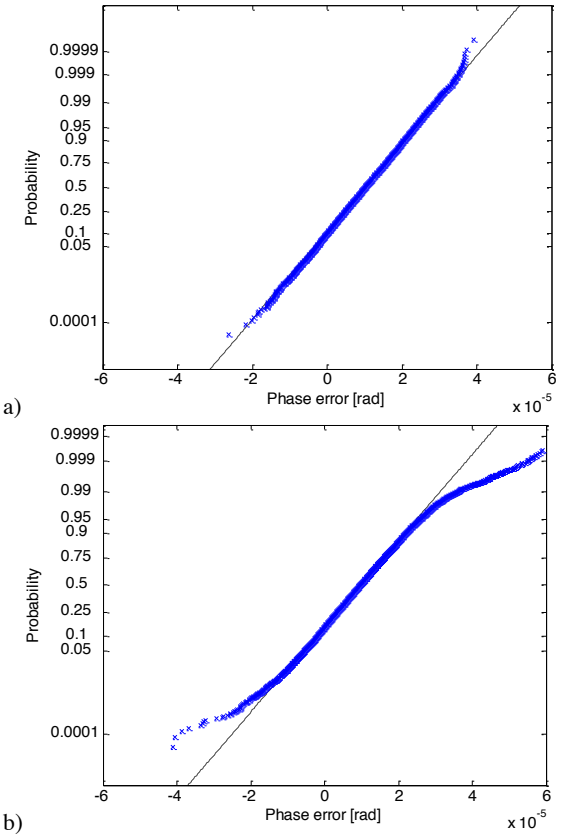

Figure 4: Experimentally inferred statistical distributions of the synchrophasor phase error: a) single tone signal, b) distorted signals with spectrum components equal to the limit values provided by the standard EN 50160 [18].

Quantity	Single tone signal	
	μ	σ
Phase error	$10.0 \cdot 10^{-6}$ [rad]	$8.1 \cdot 10^{-6}$ [rad]
RMS error	$120.0 \cdot 10^{-6}$ [p.u.]	$9.3 \cdot 10^{-6}$ [p.u.]
TVE	$117.0 \cdot 10^{-6}$	$9.3 \cdot 10^{-6}$
Frequency error	$9.0 \cdot 10^{-5}$ [Hz]	$4.5 \cdot 10^{-5}$ [Hz]
Quantity	Distorted signal	
	μ	σ
Phase error	$9.4 \cdot 10^{-6}$ [rad]	$9.9 \cdot 10^{-6}$ [rad]
RMS error	$250.0 \cdot 10^{-6}$ [p.u.]	$12.0 \cdot 10^{-6}$ [p.u.]
TVE	$250 \cdot 10^{-6}$	$12.0 \cdot 10^{-6}$
Frequency error	$9.0 \cdot 10^{-5}$ [Hz]	$3.8 \cdot 10^{-5}$ [Hz]

Table 1: Mean values and standard deviations of the error distributions of the PMU prototype with reference to steady state conditions single tone and distorted signals.

3.2 Frequency sweep representing electromechanical transients

As discussed in the literature, one of the main features of active distribution networks is that, in principle, they could allow the network exercise in islanding conditions. In this respect, distribution system operators are expected to schedule the various energy resources during their normal operation and manage unpredictable transient dynamics (e.g. [20-22]). The presence of the dispersed generation can, therefore, provide a significant improvement of the network reliability, in case the system has the capability of performing the islanding maneuver, i.e. the disconnection from the primary network, and subsequent operation in islanded mode.

Within this context, one of the main requirements of PMUs is to maintain their uncertainty levels in transient conditions so that they can provide accurate measurements to perform reliable network state estimations.

In order to determine the characteristics of the developed PMU with reference to electromechanical transients, the reference signal generator has been programmed to generate single-tone signals characterized by a frequency-sweep. In particular, the frequency has been linearly varied from 47 Hz to 53 Hz with three different ramps equal to 10 s, 30 s and 60 s.

With reference to 10 frequency sweep ramps, Fig. 5 shows the values of the standard deviations of the PMU phase and frequency error distributions as a function of the ramp time (note that different frequency ramp times result into different numbers of synchrophasor estimations).

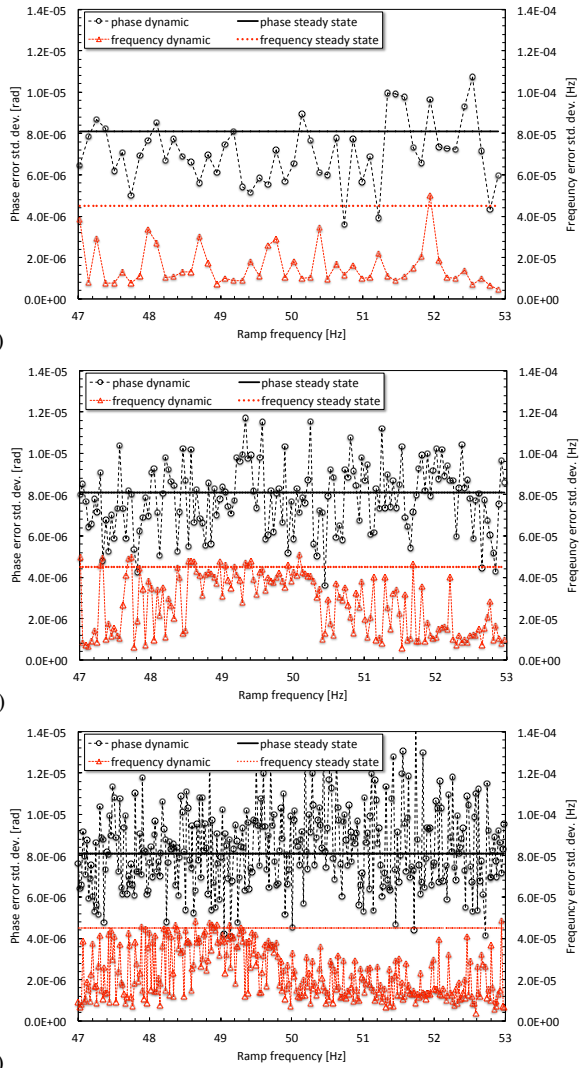

Figure 5: PMU characterization in transient conditions, standard deviations of the phase and frequency error distributions as a function of the frequency-sweep ramp time: a) 10 s frequency sweep ramp; b) 30 s frequency sweep ramp, c) 60 s frequency sweep ramp.

As it can be seen from the results of Fig. 5, even in transient conditions the developed PMU keeps its uncertainty levels to values that are the same obtained with reference to steady state signals.

3.3 Experimentally-reproduced electromechanical transient

In order to verify the robustness of the developed PMU to measure the state of a distribution network in presence of electromechanical transients, we have adopted the simplified system represented in Fig. 6 modeled within the EMTP-RV simulation environment. It consists of a 5 MVA synchronous generator, controlled by its governor, which feeds, via a step up transformer, a 15-km long overhead line at the end of which there are two loads of absorbing 2 MW and 1 MVar each. The governor of the generator is represented by a simple droop controller which transfer function is shown in Fig. 6, where K is the inverse of the permanent droop coefficient, T is the pilot time constant, $P_{m,ss}$ is the steady state mechanical power assumed to initialize the generator, P_m the set point of the mechanical power provided by the controller to the generator and Δf the frequency error. The generator field voltage is considered constant during the transient and its value is calculated on the basis of the system load flow.

The represented three-phase overhead line is composed by three 150 mm^2 aluminum-alloy conductor with a symmetrical configuration. The 50 Hz direct sequence parameters of the line are: R_d=0.226 Ω/km, X_d=0.347 Ω/km, C=10.6 nF/km, the consequent surge impedance (at 50 Hz) is Z_0=(338.7-j100.8) Ω and the propagation constant γ=(0.334+j1.124)·10^{-3} km^{-1}.

The system is initialized by assuming connected the 'Load1' only, then 'Load2' is energized after 1 s. The analog signals corresponding to the calculated phase-to-ground voltage waveforms in correspondence of nodes 'BUS_line_start' and 'BUS_line_end' of Fig. 6, are then generated by the PXI system above described and provided to two PMUs prototypes connected in correspondence of these nodes.

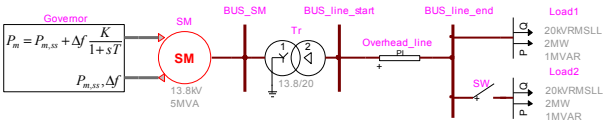

Figure 6: Simplified system adopted to verify the robustness of the developed PMU to measure the state of a distribution network in presence of electromechanical transients.

The active and reactive power flows at the beginning and at the end of the line are calculated representing the line as a two-port passive element and by using the phase-to-ground voltage synchrophasors estimated by the two PMUs.

$$
\begin{aligned}
P_{line\_start} &= -\frac{3E_{line\_start}E_{line\_end}}{B}\cos(\beta_B+\theta)+ \\
&+3E_{line\_start}^2\frac{A}{B}\cos(\beta_B-\alpha_A) \\
Q_{line\_start} &= -\frac{3E_{line\_start}E_{line\_end}}{B}\sin(\beta_B+\theta)+ \\
&+3E_{line\_start}^2\frac{A}{B}\sin(\beta_B-\alpha_A) \\
P_{line\_end} &= \frac{3E_{line\_end}E_{line\_start}}{B}\cos(\beta_B-\theta)+ \\
&-3E_{line\_end}^2\frac{A}{B}\cos(\beta_B-\alpha_A) \\
Q_{line\_end} &= \frac{3E_{line\_end}E_{line\_start}}{B}\sin(\beta_B-\theta)+ \\
&-3E_{line\_end}^2\frac{A}{B}\sin(\beta_B-\alpha_A)
\end{aligned}
\qquad (10)
$$

where:

- E_{line_start}, E_{line_end} are the RMS values of the fundamental-frequency phase-to-ground voltages synchrophasors measured by the two PMU;
- $\vartheta = \arg(\bar{E}_{line\_start}) - \arg(\bar{E}_{line\_end})$;
- $A = |\cosh\bar{\gamma}L|, B = |\bar{Z}_0 \sinh\bar{\gamma}L|$;
- $\alpha_A = \arg(\cosh\bar{\gamma}L), \beta_B = \arg(\bar{Z}_0 \cosh\bar{\gamma}L)$;

being L the line length.

Fig. 7 shows the comparison between the true and PMU-based calculated values (by means of (10)) of the active and reactive power flows in correspondence of both line terminations. Fig. 8 shows the comparison between true and PMU-measured frequency transient as well as the PMU estimated angle ϑ.

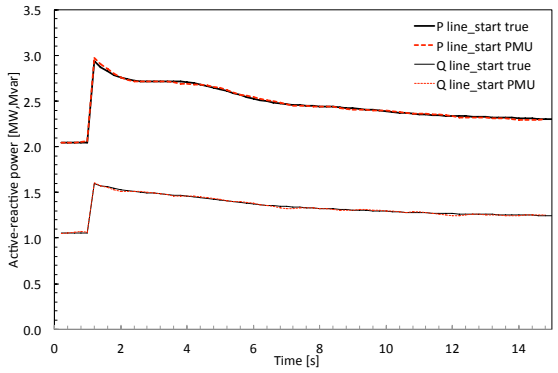

a)

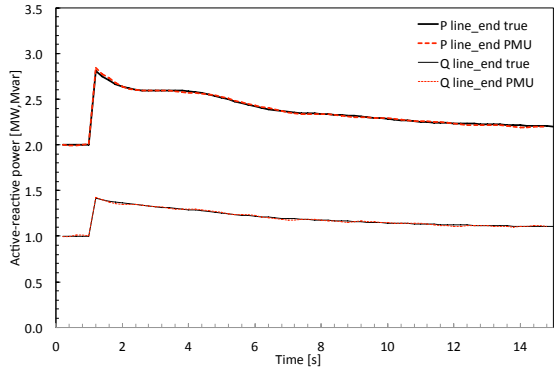

b)

Figure 7: Comparison between the true and PMU-based calculated values of the active and reactive power flows in correspondence of line start (a) and line end (b) busses of Fig. 6.

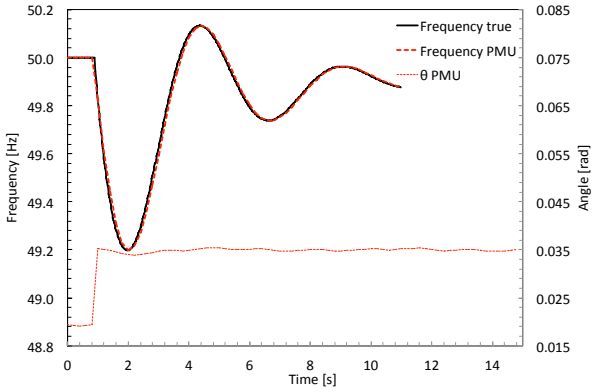

Figure 8: Comparison between the true and PMU-based calculated values of the active and reactive power flows in correspondence of line start (a) and line end (b) busses of Fig. 6.

As it can be seen from Figs 7 and 8, the power flows and the frequency transient are correctly estimated proving that the developed PMU provides data with a level of accuracy that matches the requirements of distribution networks applications even in dynamic conditions.

4 CONCLUSIONS

On the basis of previous work presented by the authors, the paper has presented an algorithm suitably developed for the synchrophasor estimation in active distribution networks. The proposed algorithm belongs to the DFT-synchrophasor estimators: it makes use of a two step approach in which the first step consists into a DFT analysis of the input signal and the second step of a specific analysis of the reconstructed time-domain signal corresponding to the fundamental-frequency tone aimed at improving the synchrophasor phase. In particular, the high sampling rate used by the algorithm has allowed an accurate identification of the fundamental tone contained into the analyzed signal and its further analysis in time domain.

The paper has also presented the algorithm implementation into an embedded real-time microcontroller as well as the procedure developed for its experimental characterization with reference to both steady state and transient conditions. The results of the experimental characterization have shown PMU accuracy levels compatible with its applications in active distribution networks. Additionally, the results have shown that the PMU accuracy levels are not influenced by the harmonic distortion of the analyzed signal and by its time-varying characteristics expressed in terms of slow frequency variations.

5 APPENDIX - INFLUENCE OF PMU ACCURACY ON THE POWER FLOWS ESTIMATION

This appendix aims at determining the influence of the synchrophasor estimation accuracy on the power flowing through a line. The line is modeled, for simplicity, by its longitudinal inductance only.

Let assume the line transposed and current flowing through line conductors ($\bar{I}_a,\bar{I}_b,\bar{I}_c$) and phase-to-ground node voltages at line start-end busses ($\bar{E}_a^{start},\bar{E}_b^{start},\bar{E}_c^{start}$, $\bar{E}_a^{end},\bar{E}_b^{end},\bar{E}_c^{end}$) only characterized by direct sequence components ($\bar{I}_d,\bar{E}_d^{start},\bar{E}_d^{end}$).

As known, the IEEE Std. C37.118 [3] limits the accuracy of the synchrophasor estimation by making reference to the Total Vector Error which is associated to both RMS and phase uncertainties of the synchrophasor estimation. In what follows we try to separate the influence of these two uncertainties on the power flows estimations.

Let ΔE and $\Delta\theta$ the RMS and phase uncertainties of the phase-to-ground voltages synchrophasors estimation performed by two PMU devices connected in correspondence of start and end busses of the line. With the above assumptions the angle between $\bar{E}_d^{start},\bar{E}_d^{end}$ is $\delta=\arg\left(\bar{E}_d^{end}\right)-\arg\left(\bar{E}_d^{start}\right)$ and the accuracy $\Delta\delta$ relevant to its estimation is $\Delta\delta=2\Delta\theta$. With the above notation, the active power flow uncertainties independently associated to ΔE and $\Delta\theta$ are:

$$\Delta P|_{\Delta E}=3\frac{\left(E_d^{start}+\Delta E\right)\left(E_d^{end}+\Delta E\right)}{X}\sin\delta-3\frac{E_d^{start}E_d^{start}}{X}\sin\delta \quad \text{(A1)}$$

$$\Delta P|_{\Delta\delta}=3\frac{E_d^{start}E_d^{start}}{X}\sin(\delta+\Delta\delta)-3\frac{E_d^{start}E_d^{start}}{X}\sin\delta \quad \text{(A2)}$$

Concerning equation (A1), let express $\Delta P|_{\Delta E}$ in per unit of the true active power flow:

$$\Delta p|_{\Delta E}=\frac{3\frac{\Delta E\left(E_d^{start}+E_d^{end}\right)}{X}\sin\delta+3\frac{\Delta E^2}{X}\sin\delta}{3\frac{E_d^{start}E_d^{end}}{X}\sin\delta} \quad \text{(A3)}$$

In equation (A3) the term with ΔE^2 can be neglected as it represents second order uncertainty value. With such an approximation, $\Delta p|_{\Delta E}$ can be approximated as

$$\Delta p|_{\Delta E}\approx\frac{\Delta E\left(E_d^{start}+E_d^{end}\right)}{E_d^{start}E_d^{end}} \quad \text{(A4)}$$

Considering that values of $\left|\bar{E}_d^{start}\right|,\left|\bar{E}_d^{end}\right|$ are, in normal operating condition of the network, very close to their rated values (E_r), $\Delta p|_{\Delta E}$ can be further approximated as

$$\Delta p|_{\Delta E}\approx\frac{2\Delta E}{E_r}=2\Delta e \quad \text{(A5)}$$

where Δe represents the per-unit value of the synchrophasor RMS uncertainty.

Concerning equation (A2), let express $\Delta P|_{\Delta\delta}$ in per unit of the true active power flow

$$\Delta p|_{\Delta\delta}=\frac{3\frac{E_d^{start}E_d^{start}}{X}\sin(\delta+\Delta\delta)}{3\frac{E_d^{start}E_d^{end}}{X}\sin\delta}-1=\frac{\sin(\delta+\Delta\delta)}{\sin\delta}-1 \quad \text{(A6)}$$

As angles δ and $\Delta\delta$ are characterized by low values, sine functions of (A6) can be approximated by their arguments, so that:

$$\Delta p|_{\Delta\delta}=\frac{\Delta\delta}{\delta}=\frac{2\Delta\theta}{\delta} \quad \text{(A7)}$$

A similar procedure can be applied to reactive power flows obtaining the following equations:

$$\Delta q^{start}\big|_{\Delta E} = \Delta q^{end}\big|_{\Delta E} = 2\Delta e \quad \text{(A8)}$$

$$\Delta q^{start}\big|_{\Delta \delta} = \Delta q^{end}\big|_{\Delta \delta} = \frac{2\Delta \theta}{\delta} \quad \text{(A9)}$$

ACKNOWLEDGEMENTS

The Authors thanks M. Peroni for the help in the experimental characterization of the PMU prototype.

REFERENCES

[1] N. Jenkins, R. Allan, P. Crossley, D. Kirschen, and G. Strbac, Embedded Generation. London, U.K.: IEE, 2000.

[2] W. Allen, "Effects of wide-area control on the protection and operation of distribution networks", Power Systems Conference, 2009. PSC 2009, pp: 1-10.

[3] IEEE Standard for Synchrophasors for Power Systems, IEEE Std. C37.118, 2005.

[4] A.G. Phadke and J.S. Thorp, Synchronized Phasor Measurements and Their Application, Springer, New York, USA, 2008.

[5] D. M. Laverty, D. J. Morrow, R. J. Best, and P. A. Crossley, "Differential ROCOF relay for loss-of-mains protection of renewable generation using phasor measurement over Internet protocol", CIGRE/IEEE Power Energy Soc. Joint Symposium Integration of Wide-Scale Renewable Resources Into the Power Delivery System, Calgary, AB, Canada, Jul. 29–31, 2009, pp. 1–7.

[6] O. Samuelsson, M. Hemmingsson, A.H. Nielsen, K.O.H. Pedersen, J. Rasmussen, "Monitoring of power system events at transmission and distribution level", IEEE Trans. Power Systems, vol. 21, no. 2, pp. 1007 1008, 2006.

[7] M. Powalko, K. Rudion, P. Komarnicki, J. Blumschein, "Observability of the distribution system", in Proc. 20th Int. Conf. and Exhib. on Electricity Distribution, CIRED, Prague, 8-11 June 2009.

[8] R.J. Best, D.J. Morrow, D. M. Laverty, and P. A. Crossley, "Synchrophasor Broadcast Over Internet Protocol for Distributed Generator Synchronization", IEEE Trans. Power Delivery, Vol. 25, No. 4, pp. 2835-2841, October 2010..

[9] A. Carta, N. Locci, and C. Muscas, "GPS-Based System for the Measurement of Synchronized Harmonic Phasors", IEEE Trans. Instrumentation and Measurement, vol. 58, no. 3, pp. 586-593, march 2009.

[10] W. Premerlani, B. Kasztenny, and M. Adamiak, "Development and implementation of a synchrophasor estimator capable of measurements under dynamic conditions," IEEE Transactions on Power Delivery, vol. 23, no. 1, pp. 109–123, Jan. 2008.

[11] A.G. Phadke and B. Kasztenny, "Synchronized Phasor and Frequency Measurement Under Transient Conditions", IEEE Trans. Power Delivery, vol. 24-1, pp. 89-95, Jan. 2009.

[12] A. Borghetti, C.A. Nucci, M. Paolone, G. Ciappi, A. Solari, "Synchronized Phasors Monitoring During the Islanding Maneuver of an Active Distribution Network", IEEE Trans. on Smart Grid, vol. 2 , issue: 1, march, 2011, pp: 70-79.

[13] J. Warichet, T. Sezi, J.-C. Maun, "Considerations about synchrophasors measurement in dynamic system conditions", Electrical Power and Energy Systems, vol. 31, 2009, pp. 452-464.

[14] A. Carta, N. Locci, C. Muscas, and S. Sulis, "A flexible GPS-based system for synchronized phasor measurement in electric distribution networks," IEEE Trans. on Instrum. and Meas., vol. 57, no. 11, Nov. 2008, pp. 2450–2456.

[15] V. Terzija, M. B. Djuric, B.D. Kovacevic, "Voltage phasor and local system frequency estimation using Newton type algorithm", IEEE Trans. on PWRD, vol. 9-3, July 1994, pp: 1368-1374.

[16] T. Grandke, "Interpolation algorithms for discrete Fourier transforms of weighted signals", IEEE Trans. Instrumentation and Measurement, vol. 32, no. 2, pp. 350-355, june 1983.

[17] V. Terzija, S.S. Wu, J. Fitch, "Setup of the laboratory for Synchronized Measurement for PMU's testing", Proc. of the 2009 IEEE Bucarest PowerTech, Bucarest, Romania, 2009, pp: 1-6.

[18] Voltage characteristics of electricity supplied by public distribution systems Std. EN 50160, CENELEC, Bruxelles, Belgium, 2004.

[19] Evaluation of measurement data - Guide to the expression of uncertainty in measurement, Joint Committee for Guides in Metrology, JCGM 100, 2008.

[20] L. Seca and J. A. Peças Lopes, "Intentional islanding for reliability improvement in distribution networks with high DG penetration", Proc. of the 2005 Int. Conference on Future Power Systems, Amsterdam, The Netherlands, 16-18 Nov. 2005.

[21] M.H.J. Bollen, Y.Sun, G.W. Ault, "Reliability of distribution networks with DER including intentional islanding", Proc. of the 2005 Int. Conference on Future Power Systems, Amsterdam, The Netherlands, 16-18 Nov. 2005.

[22] A. Borghetti, M. Bosetti, C.A. Nucci, M. Paolone, "Dispersed Energy Resources Scheduling for the Intentional Islanding Operation Of Distribution Systems", Proc. of the 16th Power Systems Computation Conf. (PSCC'08), Glasgow, Scotland, July 14-18, 2008.